This article was downloaded by: [2001:720:c20:cc05::40:111] On: 07 November 2023, At: 08:26
Publisher: Institute for Operations Research and the Management Sciences (INFORMS)
INFORMS is located in Maryland, USA

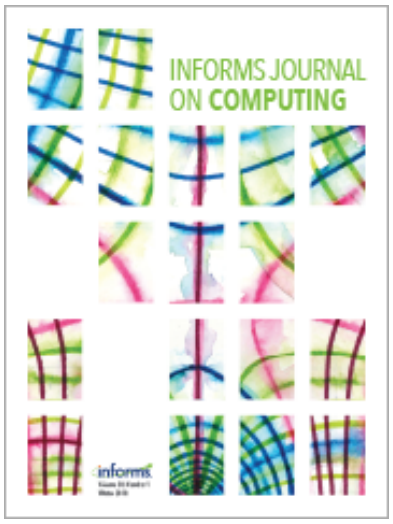

INFORMS Journal on Computing

Publication details, including instructions for authors and subscription information:
http://pubsonline.informs.org

Tight and Compact Sample Average Approximation for Joint Chance-Constrained Problems with Applications to Optimal Power Flow

Álvaro Porras, Concepción Domínguez, Juan Miguel Morales, Salvador Pineda

To cite this article:
Álvaro Porras, Concepción Domínguez, Juan Miguel Morales, Salvador Pineda (2023) Tight and Compact Sample Average Approximation for Joint Chance-Constrained Problems with Applications to Optimal Power Flow. INFORMS Journal on Computing

Published online in Articles in Advance 02 Aug 2023

. https://doi.org/10.1287/ijoc.2022.0302

Full terms and conditions of use: https://pubsonline.informs.org/Publications/Librarians-Portal/PubsOnLine-Terms-and-Conditions

This article may be used only for the purposes of research, teaching, and/or private study. Commercial use or systematic downloading (by robots or other automatic processes) is prohibited without explicit Publisher approval, unless otherwise noted. For more information, contact permissions@informs.org.

The Publisher does not warrant or guarantee the article's accuracy, completeness, merchantability, fitness for a particular purpose, or non-infringement. Descriptions of, or references to, products or publications, or inclusion of an advertisement in this article, neither constitutes nor implies a guarantee, endorsement, or support of claims made of that product, publication, or service.

Copyright © 2023 The Author(s)

Please scroll down for article—it is on subsequent pages

With 12,500 members from nearly 90 countries, INFORMS is the largest international association of operations research (O.R.) and analytics professionals and students. INFORMS provides unique networking and learning opportunities for individual professionals, and organizations of all types and sizes, to better understand and use O.R. and analytics tools and methods to transform strategic visions and achieve better outcomes.
For more information on INFORMS, its publications, membership, or meetings visit http://www.informs.org

https://pubsonline.informs.org/journal/ijoc

INFORMS JOURNAL ON COMPUTING
Articles in Advance, pp. 1–16
ISSN 1091-9856 (print), ISSN 1526-5528 (online)

Downloaded from informs.org by [2001:720:c20:cc05::40:111] on 07 November 2023, at 08:26 . For personal use only, all rights reserved.

Tight and Compact Sample Average Approximation for Joint Chance-Constrained Problems with Applications to Optimal Power Flow

Álvaro Porras,[a] Concepción Domínguez,[a] Juan Miguel Morales,[a,*] Salvador Pineda[a]

[a] OASYS Research Group, University of Málaga, 29071 Málaga, Spain

*Corresponding author

Contact: alvaroporras19@gmail.com, https://orcid.org/0000-0002-3956-9996 (ÁP); concepcion.dominguez@uma.es, https://orcid.org/0000-0002-9046-4997 (CD); juan.morales@uma.es, https://orcid.org/0000-0002-9114-686X (JMM); spinedamorente@gmail.com, https://orcid.org/0000-0002-1089-0970 (SP)

Received: February 21, 2023
Revised: June 8, 2023; June 16, 2023
Accepted: June 21, 2023
Published Online in Articles in Advance: August 2, 2023

https://doi.org/10.1287/ijoc.2022.0302

Copyright: © 2023 The Author(s)

Abstract. In this paper, we tackle the resolution of chance-constrained problems reformulated via sample average approximation. The resulting data-driven deterministic reformulation takes the form of a large-scale mixed-integer program (MIP) cursed with Big-Ms. We introduce an exact resolution method for the MIP that combines the addition of a set of valid inequalities to tighten the linear relaxation bound with coefficient strengthening and constraint screening algorithms to improve its Big-Ms and considerably reduce its size. The proposed valid inequalities are based on the notion of k-envelopes and can be computed off-line using polynomial-time algorithms and added to the MIP program all at once. Furthermore, they are equally useful to boost the strengthening of the Big-Ms and the screening rate of superfluous constraints. We apply our procedures to a probabilistically constrained version of the DC optimal power flow problem with uncertain demand. The chance constraint requires that the probability of violating any of the power system's constraints be lower than some positive threshold. In a series of numerical experiments that involve five power systems of different size, we show the efficiency of the proposed methodology and compare it with some of the best performing convex inner approximations currently available in the literature.

History: Accepted by Andrea Lodi, Area Editor for Design & Analysis of Algorithms – Discrete.

Open Access Statement: This work is licensed under a Creative Commons Attribution 4.0 International License. You are free to copy, distribute, transmit and adapt this work, but you must attribute this work as "*INFORMS Journal on Computing*. Copyright © 2023 The Author(s). https://doi.org/10.1287/ijoc.2022.0302, used under a Creative Commons Attribution License: https://creativecommons.org/licenses/by/4.0/."

Funding: This work was supported in part by the European Research Council under the EU Horizon 2020 research and innovation program [Grant 755705], in part by the Spanish Ministry of Science and Innovation [Grant AEI/10.13039/501100011033] through project PID2020-115460GB-I00, and in part by the Junta de Andalucía and the European Regional Development Fund through the research project P20_00153. Á. Porras is also financially supported by the Spanish Ministry of Science, Innovation and Universities through the University Teacher Training Program with fellowship number FPU19/03053.

Supplemental Material: The online supplement is available at https://doi.org/10.1287/ijoc.2022.0302.

Keywords: chance constraints • probabilistic constraints • k-violation problems • combinatorial optimization • mixed-integer programming • valid inequalities • optimal power flow

1. Introduction

Chance-constrained programming suits applications in areas in which decisions have to be made dealing with random parameters (Miller and Wagner 1965). In these situations, it is desirable to ensure feasibility of the system almost surely, but there is hardly any decision that would guarantee it under extreme events or unexpected random circumstances. Within this context, chance-constrained programming offers a powerful modeling framework to identify cost-efficient decisions that satisfy the problem's constraints with a high level of confidence.

In this paper, we focus on chance-constrained problems (CCPs) with joint linear chance constraints and random right-hand side (RHS) and left-hand side (LHS), that is,

$$\min_{x} \quad f(x) \tag{1a}$$

$$\text{s.t.} \quad x \in X, \tag{1b}$$

$$\mathbb{P}\{a_j(\omega)^\top x \leqslant b_j(\omega), \quad \forall j \in \mathcal{J}\} \geqslant 1-\epsilon. \tag{1c}$$

Downloaded from informs.org by [2001:720:c20:cc05::40:111] on 07 November 2023, at 08:26 . For personal use only, all rights reserved.

In (1), $x \in \mathbb{R}^{|\mathcal{I}|}$ is a vector of continuous decision variables, $X \subseteq \mathbb{R}^{|\mathcal{I}|}$ represents a set of deterministic constraints, and $f : \mathbb{R}^{|\mathcal{I}|} \to \mathbb{R}$ is a convex function. Uncertainty is represented through the random vector ω taking values in $\mathbb{R}^d$ and giving rise to a technology matrix with random rows $a_j(\omega) \in \mathbb{R}^{|\mathcal{I}|}$, $j \in \mathcal{J}$ and random $b_j(\omega) \in \mathbb{R}$, $j \in \mathcal{J}$. $\mathbb{P}$ is a probability measure, and ϵ is a confidence or risk parameter, typically near zero, so that the set of Constraints (1c) are satisfied with probability at least $(1-\epsilon)$. Apart from power systems, applications of CCPs include supply chain, location and logistics (Taleizadeh et al. 2012, Shaw et al. 2016, Elçi et al. 2018), risk control in finance (Daníelsson et al. 2008, Natarajan et al. 2008), and healthcare problems such as operating room planning (Najjarbashi and Lim 2020) or vaccine allocation (Tanner et al. 2008), among others.

When the probabilistic constraint corresponds to (1c), the CCP has joint chance constraints (JCC) and is, hence, classified as a joint CCP (JCCP) in contrast with single CCPs (SCCPs), that is, CCPs with individual or single chance constraints (SCC) of the form $\mathbb{P}\{a_j(\omega)^\top x - b_j(\omega) \leqslant 0\} \geqslant 1-\epsilon_j,\ \forall j \in \mathcal{J}$. JCCPs are suitable for contexts in which all constraints need to be simultaneously satisfied with a high probability, and the dependence between random variables makes them clearly harder. Both SCCPs and JCCPs are extensively studied (see Prékopa 2003, Van Ackooij et al. 2011, and the references therein).

There are a number of reasons why general CCPs are challenging. The first one is the nonconvexity of the feasible set. In general, the feasible region of a CCP is not convex in the original space even when x is continuous, there is only RHS uncertainty, and the constraints inside the probability in (1c) define a polyhedral region (Küçükyavuz and Jiang 2022). To circumvent this problem, several approaches are proposed. Some methods (e.g., Lagoa et al. 2005, Henrion 2007, Henrion and Strugarek 2011) give convexity results and investigate the conditions under which the feasible region of Problem (1) is convex. In another line of research, various convex approximation schemes, such as quadratic (Ben-Tal and Nemirovski 2000) or Bernstein approximation (Nemirovski and Shapiro 2007), are proposed in the literature. The conditional value at risk (CVaR) approximation has gained a lot of popularity since its introduction (Rockafellar and Uryasev 2000, Sun et al. 2014) and remains one of the most used methods to deal with stochastic problems. Nonetheless, the solutions to the approximated problems err on the side of overconservatism. In this context, some iterative schemes such as ALSO-X have been recently proposed to identify tighter inner convex approximations of the CCP at the expense of a higher computational cost (Ahmed et al. 2017, Jiang and Xie 2022). Finally, other works suggest convex approximations for nonlinear CCPs. For instance, Hong et al. (2011) propose to solve the JCCP by a sequence of convex approximations followed by a gradient-based Monte Carlo method, whereas Peña-Ordieres et al. (2020) introduce a smooth sampling-based approximation.

The second difficulty of CCPs is that checking the feasibility of a given solution is not, in general, an easy task. For instance, even if the uncertainty follows a known continuous distribution, calculating the joint probability requires a multidimensional integration, which becomes increasingly difficult with the dimension of the random vector ω. On top of that, in most cases, the distribution $\mathbb{P}$ is not fully known.

A commonly used approach to cope with these obstacles is to replace $\mathbb{P}$ with its empirical estimate based on a set of random samples (Shapiro 2003). This approach is known in the technical literature as sample average approximation (SAA) and may also be seen as a data-driven approach that works with observations of ω that are available to the decision maker even if the true data-generating distribution $\mathbb{P}$ is unknown. The main advantage of SAA is that it allows us to reformulate CCPs as deterministic optimization problems that can be solved using standard optimization techniques.

Indeed, the deterministic reformulation of (1) using SAA results in a mixed-integer problem (MIP). For the resolution of CCPs using MIP reformulations, we refer the reader to Küçükyavuz and Jiang (2022). When there is only RHS uncertainty (i.e., the technology matrix is fixed), a reformulation of the problem leads to an MIP with a set of constraints that form a mixing set and that has been extensively studied alone or in combination with the knapsack constraint that also appears in the formulation (Günlük and Pochet 2001, Luedtke et al. 2010, Abdi and Fukasawa 2016). Alternative reformulations such as the ones proposed by Dentcheva et al. (2000) and Nair and Miller-Hooks (2011) rely on the concept of $(1-\epsilon)$-efficient points. The case when the technology matrix is random, whereas the RHS is not, is studied, for example, in Tayur et al. (1995). As for the general case, it is also addressed in the literature. Specifically, a large line of research focuses on the development of quantile cuts, a particular type of valid inequality that can be viewed as a projection of a set of mixing inequalities for the MIP onto the original problem space. These cuts and the associated quantile closure are recently studied in Qiu et al. (2014), Xie and Ahmed (2016, 2018), and Ahmed and Xie (2018) and successfully applied to computational experiments of CCPs in Song et al. (2014) and Ahmed et al. (2017), among others.

Regarding its disadvantages, the SAA solution tends to be optimistic and underestimate the probability of violating the constraints (Nemirovski and Shapiro 2006). In fact, the performance of SAA is directly contingent on the number of samples available. We refer the reader to the article by Luedtke and Ahmed (2008), in which relations are established between the empirical acceptable probability of violation and the number of samples such

Downloaded from informs.org by [2001:720:c20:cc05::40:111] on 07 November 2023, at 08:26 . For personal use only, all rights reserved.

that the SAA-based solution be feasible in the JCCP with a predefined confidence level. In this paper, however, we do not investigate how well the SAA-based solution approximates the solution of the original JCCP. Statistical considerations apart, the main focus of this paper is on proposing an efficient methodology to solve the deterministic optimization model that results from reformulating JCCPs using SAA. In particular, the method we propose solves the MIP to optimality and is based on the combination of a tightening-and-screening procedure with the development of valid inequalities to obtain a formulation that is compact and tight at a time.

We begin with a description of an iterative algorithm to strengthen the Big-Ms present in the mixed-integer reformulation of the JCC. Interestingly, although the procedure is not new (see Qiu et al. 2014), we complement it with a screening procedure that allows us to eliminate inequalities of the MIP.

Next, we introduce a new set of valid inequalities designed to strengthen the linear relaxation of the model. As for their structure, each valid inequality is developed using quantile information and avoiding the use of Big M constants, which are known to lead to weak linear relaxation bounds. Furthermore, from a theoretical point of view, they are closely related to the aforementioned quantile cuts. In fact, as proven in Online Section EC.1, the addition of our inequalities yields a feasible region equivalent to the quantile closure of a specific relaxation of the MIP problem. The main advantage of our inequalities is that, unlike quantile cuts, they are not NP-hard to compute, and neither do they require a specific separation algorithm to include them dynamically (that is, they can all be included in the model from the outset). As many other techniques developed for JCCPs, our cuts also apply to the SCCPs. Finally, our valid inequalities extend the results introduced in Roos and Widmayer (1994) for the k-violation problem, which can be seen as a mixed-integer linear problem reformulation of a SCCP. For ease of explanation, the valid inequalities are proposed for a particular class of linear chance constraints, but our results are also applicable to more general types of CCPs as we detail in Online Section EC.2.

We apply our resolution method to the optimal power flow (OPF) problem for which we propose a chance-constrained formulation and extensive computational experiments featuring results for five standard power systems available in the literature. The combination of the valid inequalities with the tightening of the Big-Ms and the screening procedure allows us to effectively solve to optimality instances that are not solved with the initial MIP formulation because the combination of both techniques notably reduces their size and difficulty. We also compare our resolution approach with state-of-the-art convex inner approximations of CCPs, in particular, the CVaR-based approximation, ALSO-X, and ALSO-X+ (Jiang and Xie 2022). Finally, we compare our results with an exact approach for solving CCPs assuming SAA, namely, the branch-and-cut decomposition algorithm proposed in Luedtke (2014). This algorithm is based on the addition of quantile cuts strengthened using the star inequalities of Atamtürk et al. (2000) to a relaxation of the original problem.

The remainder of the paper is organized as follows. Section 2 involves the reformulation of the problem into an MIP using SAA and the proposed methodology: Section 2.1 describes the tightening and screening procedures, whereas Section 2.2 introduces the valid inequalities and the necessary algorithms to compute them. Section 3 is devoted to the application of the results to the OPF problem. The section begins with an introduction to the problem and the associated literature review, and Section 3.1 formalizes the notation and the mathematical model solved in the computational study. In Section 3.2, we present the case study, testing our results to solve instances of the direct current (DC) OPF available in the literature. Section 4 points to further research topics and includes some concluding remarks. Finally, the main text is accompanied by an online supplement, in which Section EC.1 establishes the relationship between our valid inequalities and the quantile cuts present in the literature and Section EC.2 details the complexity of the algorithms proposed in Section 2.2 and discusses the generalization of our methodology and its possible application to other types of CCPs.

2. Solving JCCPs via Sample Average Approximation

Using SAA, Problem (1) can be reformulated into an MIP. To this aim, assume that ω has a finite discrete support defined by a collection of points $\{\omega_s \in \mathbb{R}^{|\mathcal{N}|}, s \in \mathcal{S}\}$ and respective probability masses $\mathbb{P}(\omega = \omega_s) = (1/|\mathcal{S}|),\ \forall s \in \mathcal{S} = \{1, \ldots, |\mathcal{S}|\}$. Consider the rows $a_{js} = a_j(\omega_s)$ and the random $b_{js} = b_j(\omega_s)$. Define $p := \lfloor \epsilon|\mathcal{S}| \rfloor$, the vector y of binary variables y_s, $\forall s \in \mathcal{S}$, and the large enough constants M_{js}. Then, the MIP reformulation of Problem (1) can be stated as

$$\min_{x} \quad f(x) \tag{2a}$$

$$\text{s.t.} \quad x \in X, \tag{2b}$$

$$a_{js}^{\top} x \leqslant b_{js} + M_{js} y_s, \quad \forall j \in \mathcal{J}, s \in \mathcal{S}, \tag{2c}$$

$$\sum_{s \in \mathcal{S}} y_s \leqslant p, \tag{2d}$$

$$y_s \in \{0,1\}, \quad \forall s \in \mathcal{S}. \tag{2e}$$

Downloaded from informs.org by [2001:720:c20:cc05::40:111] on 07 November 2023, at 08:26 . For personal use only, all rights reserved.

Using the generic formulation (2), we present in Section 2.1 a procedure to properly tune the values of the large constants M_{js}. We also explain in this section how the intermediate results of the tightening procedure can be efficiently used to remove constraints from Set (2c) that are superfluous, thus making Model (2) more compact. Finally, we introduce in Section 2.2 a set of valid inequalities that makes the linear relaxation of a particular case of (2) remarkably tighter, and we relate our inequalities to the quantile closure studied in Xie and Ahmed (2018).

2.1. Tightening and Screening

It is well known that the linear relaxation of a Big M formulation tends to provide weak lower bounds in general (Conforti et al. 2014). This is even more so when the Big-Ms are chosen too loose. Constants M_{js} in (2c) should be set large enough for the corresponding constraints to be redundant when the associated binary variables y_s are equal to one and as small as possible to tighten the MIP formulation. To this end, Qiu et al. (2014) provide an algorithm called iterative coefficient strengthening that has been successfully applied to other CCPs (see, e.g., Song et al. 2014). A customization of this procedure for the joint chance-constrained formulation (2) is detailed in Algorithm 1.

Algorithm 1 (Iterative Coefficient Strengthening)

Input: The LHS and RHS vectors $\{a_{js}\}_{j\in\mathcal{J},s\in\mathcal{S}}$ and coefficients $\{b_{js}\}_{j\in\mathcal{J},s\in\mathcal{S}}$, respectively, and the maximum allowed violation probability p that determine the joint chance-constraint system (2d), the deterministic feasible set X, and the total number of iterations κ.

Output: The large constants M_{js}, $\forall j\in\mathcal{J}$, $s\in\mathcal{S}$.

Step 1. Initialization, $k=0$, $M^0_{js}=\infty$, $\forall j\in\mathcal{J}$, $s\in\mathcal{S}$.

Step 2. For each $j\in\mathcal{J}$ and $s\in\mathcal{S}$ update M^{k+1}_{js} as follows: If $M^k_{js}<0$, then $M^{k+1}_{js}=M^k_{js}$. Otherwise,

$$M^{k+1}_{js}=\max_{x,y_s} \quad a_{js}^\top x-b_{js} \tag{3a}$$

$$\text{s.t.} \quad x\in X, \tag{3b}$$

$$a_{js}^\top x-b_{js}\leqslant M^k_{js}y_s, \quad \forall j\in\mathcal{J},s\in\mathcal{S}, \tag{3c}$$

$$\sum_{s\in\mathcal{S}} y_s\leqslant p, \tag{3d}$$

$$0\leqslant y_s\leqslant 1, \quad \forall s\in\mathcal{S}. \tag{3e}$$

Step 3. If $k+1<\kappa$, then $k=k+1$ and go to step 2. Otherwise, stop.

The output of Algorithm 1 is the tuned Big-Ms that are input to the MIP reformulation (2). This algorithm produces Big-Ms whose value either decreases or remains equal at each iteration. There are, in fact, a number of iterations beyond which the resulting Big-Ms converge. To reduce the computational burden of running Algorithm 1, all Problems (3) in step 2 can be solved in parallel. Hereinafter, we use the short name "**T**(κ)" (from "tightening") to refer to the solution of Model (2) using the Big M values given by the iterative coefficient strengthening algorithm with κ iterations.

Equally important, Algorithm 1 can be easily upgraded to delete constraints (j, s) in (2c) that are redundant and, therefore, can be removed from Problem (2). Indeed, if Algorithm 1 delivers a large constant $M_{js}\leqslant 0$, then constraint j in scenario s can be deleted from (2) without altering its feasible region or its optimal solution. This is so because a nonpositive M_{js} means that there is no x satisfying (3b)–(3e) such that the constraint takes on a value strictly greater than zero. Consequently, the constraint is redundant in (2) because the feasibility region of (3) is a relaxation of (2). This upgrade of method **T** not only makes Formulation (2) tighter through coefficient strengthening, but also more compact by screening out redundant constraints. Naturally, the tightening and screening power of algorithm **T** increases at each iteration. From now on, we use the short name "**TS**(κ)" (from "tightening and screening") to refer to the strategy whereby Model (2) is solved without the Constraints (2c) for which the value of M_{js} provided by Algorithm 1 after κ iterations is lower than or equal to zero.

Whereas strengthening the parameters M_{js} is a common strategy in the technical literature to reduce the computational burden of CCPs, this is the first time, to our knowledge, that intermediate results of Algorithm 1 are used to eliminate superfluous constraints from Model (2). We stress that the screening process itself comes at no cost from Algorithm 1, whereas removing superfluous constraints from (2) may substantially facilitate its solution. As we show in Section 3.2, this is particularly true for the JCC-OPF.

Apart from making Formulation (2) more compact, the screening of superfluous constraints can also be used to accelerate the iterative coefficient strengthening process at each iteration. To do so, it suffices to modify

Downloaded from informs.org by [2001:720:c20:cc05::40:111] on 07 November 2023, at 08:26 . For personal use only, all rights reserved.

Algorithm 1 so that (3c) only includes the constraints for which $M^k_{js} > 0$. Thus, the number of constraints of Model (3) is significantly reduced, and so is its solution time.

2.2. Valid Inequalities

In this section, we propose valid inequalities that apply to JCCPs with a particular structure: each row $a_j(\omega)$ in the technology matrix of (1) can be rewritten as $a_j(\omega) = a^0_j + \Omega_j(\omega)\hat{a}_j$ with $a^0_j, \hat{a}_j \in \mathbb{R}^{|\mathcal{I}|}$ and in which $\Omega_j(\omega_s) = \Omega_{js}$ is a real-valued function whose domain includes the support of ω. In other words, we derive a set of valid inequalities to make the linear relaxation of problem

$$\min_{x, y_s} \quad f(x) \tag{4a}$$

$$\text{s.t.} \quad x \in X, \tag{4b}$$

$$\Omega_{js}\hat{a}_j^\top x - b_{js} + x^\top a^0_j \leqslant M_{js} y_s, \quad \forall j \in \mathcal{J}, s \in \mathcal{S}, \tag{4c}$$

$$\sum_{s \in \mathcal{S}} y_s \leqslant p, \tag{4d}$$

$$y_s \in \{0,1\}, \quad \forall s \in \mathcal{S} \tag{4e}$$

tighter. Note that we do not make any assumptions on the sign of $\hat{a}_j^\top$, b_{js}, and a^0_j. Furthermore, these valid inequalities can also be added to the constraint set (3) of Algorithm 1, thus dramatically increasing the tightening and screening power of **TS**. To facilitate the comparative analysis carried out in Section 3.2, the so upgraded algorithm is named "**TS+V**(κ)" (from "tightening and screening with valid inequalities").

To derive the set of valid inequalities for Problem (4), we define the real variables $z_j \in \mathbb{R}$ as $z_j := \hat{a}_j^\top x$ and let $z^d_j = \inf_{x \in X} \hat{a}_j^\top x$, $z^u_j = \sup_{x \in X} \hat{a}_j^\top x$ denote the lower and upper bounds on z induced by the feasibility set (4b). Let us also define the function $L_{js} : f_{js}(z_j) = \Omega_{js} z_j - b_{js}$ for $z_j \in [z^d_j, z^u_j]$ and the set of functions $\mathcal{L}_j := \{L_{js}, \ \forall s \in \mathcal{S}\}$. The valid inequalities we propose are heavily supported by the concepts of k-lower and k-upper envelopes, which we define in the following.

Definition 1. For a given line L_{js}, we say that the point $(\tilde{z}, \tilde{t}) \in \mathbb{R}^2$ lies below, on, or above function L_{js} depending on whether $\tilde{t} < \Omega_{js}\tilde{z} - b_{js}$, $\tilde{t} = \Omega_{js}\tilde{z} - b_{js}$, or $\tilde{t} > \Omega_{js}\tilde{z} - b_{js}$, respectively. Naturally, we also say that function L_{js} lies above, contains, or lies below point $(\tilde{z}, \tilde{t})$ in these cases. We also say that a point $(\tilde{z}, \tilde{t})$ belongs to the set of lines $\mathcal{L}_j$ if there exists a line $L_{js} \in \mathcal{L}_j$ that contains the point $(\tilde{z}, \tilde{t})$.

Definition 2. For a set of lines $\mathcal{L}_j$, the lower (respectively, upper) score of a point is the number of lines in $\mathcal{L}_j$ that lie below (above) that point. The k-lower (k-upper) envelope of a set of lines $\mathcal{L}_j$ is the closure of the set of points that belong to $\mathcal{L}_j$ and that have lower (upper) score equal to $k - 1$. The k-lower envelope is also known as k-level.

For the sake of illustration, Figure 1 shows in bold the five-upper envelope of a set of eight lines. Clearly, the k-envelopes of sets $\mathcal{L}_j$ can be seen as piecewise linear functions on z_j.

Figure 1. Example of a k-upper Envelope

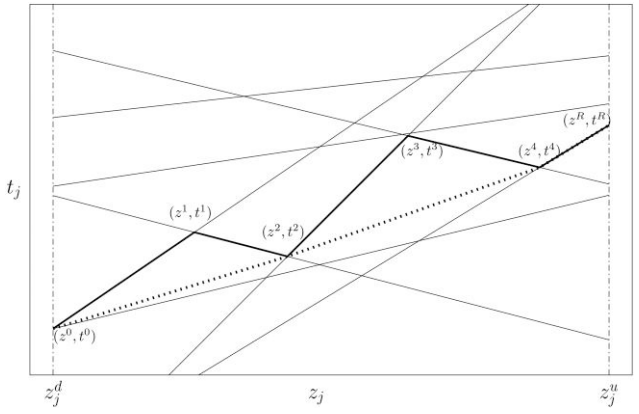

Notes. In bold, the five-upper envelope (four-lower envelope, four-level) of a set $\mathcal{L}_j$ of eight lines in the plane. In dotted, the lower hull of the five-upper envelope.

Downloaded from informs.org by [2001:720:c20:cc05::40:111] on 07 November 2023, at 08:26 . For personal use only, all rights reserved.

Proposition 1. *For a fixed $j \in \mathcal{J}$, let $U_j^{p+1}(\cdot)$ be the $(p+1)$-upper envelope of the set of lines $\mathcal{L}_j$ with $p := \lfloor \epsilon |\mathcal{S}| \rfloor$. Then, the inequality*

$$U_j^{p+1}(\hat{a}_j^\top x) + x^\top a_j^0 \leqslant 0, \quad x \in X \tag{5}$$

is valid for Problem (4).

Proof. Let $\overline{x}, \overline{y}$ be any feasible solution of Problem (4) with $\overline{z}_j = \hat{a}_j^\top \overline{x} \in [z_j^d, z_j^u]$ and suppose that $U_j^{p+1}(\overline{z}_j) + \overline{x}^\top a_j^0 > 0$. By definition of k-upper envelope, there exist $p+1$ lines in $\mathcal{L}_j$, $L_{js_i} : f_{js_i}(z_j) = \Omega_{js_i} z_j - b_{js_i}$ $\forall i \in \{1, \ldots, p+1\}$ such that $f_{js_i}(\overline{z}_j) = \Omega_{js_i}\overline{z}_j - b_{js_i} \geqslant U_j^{p+1}(\overline{z}_j)$. Then, for $i \in \{1, \ldots, p+1\}$ it holds that $\Omega_{js_i}\overline{z}_j - b_{js_i} + \overline{x}^\top a_j^0 > 0$. Substituting in Constraint (4c), we obtain that $\overline{y}_{s_i} M_{s_i} > 0 \Rightarrow \overline{y}_{s_i} = 1$ for $i \in \{1, \ldots, p+1\}$. But then Constraint (4d) is not satisfied because $\sum_{s \in \mathcal{S}} \overline{y}_s \geqslant \sum_{i=1}^{p+1} \overline{y}_{s_i} = p+1 > p$. This is, however, in contradiction with our initial statement that $\overline{x}, \overline{y}$ is a feasible solution of Problem (4). □

The technical literature already includes references that propose methodologies to determine the k-envelope of a set of linear functions. For instance, Cheema et al. (2014) give a basic algorithm for constructing k-envelopes called the rider algorithm. Essentially, this algorithm is based on the fact that the k-envelope is an unbounded polygonal chain that can be described by a sequence of vertices, which are intersections of lines of the set. In fact, every point in the k-envelope is contained in a given line. In this paper, we adapt the algorithm proposed in Cheema et al. (2014) to the particular case in which z_j^d, z_j^u are finite. Algorithm 2 describes our procedure in detail for a general set of the type $\mathcal{L}_j$.

Algorithm 2 (Rider Algorithm to Build the k-Upper Envelope of $\mathcal{L}_j$ (Adapted to the Bounded Case))

To describe the k-upper envelope of a set of lines $\mathcal{L}_j$, we derive the sequence of vertices of the polygonal chain (intersections of lines in $\mathcal{L}_j$) $((z^0, t^0), \ldots, (z^R, t^R))$ with $(z_j^d = z^0 < \ldots < z^R = z_j^u)$.

Step 1. Set $r = 0$. Let $\{(z_j^d, \Omega_{js} z_j^d - b_{js}), \forall s \in \mathcal{S}\}$, be the intersections of the lines $L_{js} \in \mathcal{L}_j$ with the vertical line $z = z_j^d$ and assume without loss of generality that all the points have different upper scores. Let $s_0 \in \mathcal{S}$ be such that the intersection $(z_j^d, \Omega_{js_0} z_j^d - b_{js_0})$ has an upper score equal to $k-1$. Then, $(z^0, t^0) = (z_j^d, \Omega_{js_0} z_j^d - b_{js_0})$.

Step 2. Compute the value of z_j for which the line L_{js_r} intersects the rest of the lines $L_{js} \in \mathcal{L}_j$ as $\text{int}_z(s, s_r) = (b_{js} - b_{js_r})/(\Omega_{js} - \Omega_{js_r})$. If $\exists\, s', z^r < \text{int}_z(s', s_r) < z^u$, go to step 3. Otherwise, go to step 4.

Step 3. Find the line that intersects L_{js_r} at the leftmost point to the right of z^r, that is, find $s_{r+1} = \text{argmin}_s\{\text{int}_z(s, s_r) \;\; : \text{int}_z(s, s_r) > z^r\}$. Set $(z^{r+1}, t^{r+1}) = (\text{int}_z(s_{r+1}, s_r), \Omega_{js_r} \text{int}_z(s_{r+1}, s_r) - b_{js_r})$, update $r = r+1$, and go to step 2.

Step 4. Set $(z^R, t^R) = (z_j^u, \Omega_{js_r} z_j^u - b_{js_r})$.

The LHSs of the valid inequalities (5) are piecewise linear functions not necessarily convex. Therefore, the inclusion of these inequalities into Model (4) requires a significant amount of additional binary variables, which, in turn, is expected to increase the computational burden of this problem even further. Alternatively, we compute the lower hull of the k-upper envelope of $\mathcal{L}_j$, which takes the form of a convex piecewise linear function. From this lower hull, we can extract a set of linear valid inequalities (the linear extensions of the pieces) that can be seamlessly inserted into Model (4) without the need of any extra binary variables. In doing so, we are able to tighten Model (4), which can, thus, be solved more efficiently by available optimization software. Before presenting the set of valid inequalities, the following definition is required.

Definition 3. Let Z be the convex hull of a set of points P. The upper (lower) hull of P is the set of edges of Z that lie on or above (on or below) every point in P.

Corollary 1 presents the set of linear valid inequalities (6) given by the lower hull of the k-upper envelope of $\mathcal{L}_j$.

Corollary 1. *Let $\{(z^r, t^r)\}$, $r \in \{0, \ldots, R\}$, be the ordered set of vertices obtained by applying Algorithm 2 to set $\mathcal{L}_j$, and let $\{(z^{r'}, t^{r'})\}$, $r' \in \{0, \ldots, R'\} \subseteq \{0, \ldots, R\}$, be the ordered subset of vertices such that the associated polygonal chain is the lower hull. Then, the following linear inequalities*

$$\frac{t^{r'+1} - t^{r'}}{z^{r'+1} - z^{r'}} (\hat{a}_j^\top x - z^{r'}) + t^{r'} \leqslant -x^\top a_j^0, \quad x \in X, r' \in \{0, \ldots, R'-1\} \tag{6}$$

are valid for Problem (4).

Downloaded from informs.org by [2001:720:c20:cc05::40:111] on 07 November 2023, at 08:26 . For personal use only, all rights reserved.

Proof. The proof is straightforward because, for each $x \in X$, it holds

$$\frac{t^{r'+1} - t^{r'}}{z^{r'+1} - z^{r'}}(\hat{a}_j^\top x - z^{r'}) + t^{r'} \leqslant U_j^{p+1}(\hat{a}_j^\top x) \leqslant -x^\top a_j^0$$

by hypothesis and using (5). □

There exist plenty of algorithms of convexification of a set of points in the plane. Two of the most well-known are the Jarvis march and the Graham scan (Tóth et al. 2017). Here, we give a simplified version of the former in which we make use of special features of our set of points and only compute the lower hull. In particular, we assume that we have a set of presorted points $\{(z^r, t^r)\}$, $r \in \{0, \dots, R\}$ whose first and last points always belong to the hull. To speed up the process, we can find the point $(z^{\bar{r}}, t^{\bar{r}})$ from the previous set with the lowest t-coordinate (which always belongs to the lower hull) and then apply the algorithm to the subsets $\{(z^0, t^0), \dots, (z^{\bar{r}}, t^{\bar{r}})\}$ and $\{(z^{\bar{r}}, t^{\bar{r}}), \dots, (z^R, t^R)\}$. Algorithm 3 describes in detail the proposed convexification procedure.

Algorithm 3 (Jarvis March Algorithm to Obtain the Lower Hull of a Set of Presorted Points P)
Let $P = \{(z^r, t^r)\}$, $r \in \{0, \dots, R\}$ be a set of points with $z^0 < \cdots < z^R$. The algorithm derives a subset $P' = \{(z^{r'}, t^{r'})\}$, $r' \in \{0, \dots, R'\} \subseteq \{0, \dots, R\}$, which constitutes the lower hull of the first set.

Step 1. Initially, set $P' = \{(z^0, t^0)\}$.

Step 2. Assume $(z^{r'}, t^{r'})$ is the last point included in P'. If $r' = R$, the lower hull of P is given by the set of points P'. Otherwise, let $r' + 1 := \operatorname{argmin}_r\{(t^r - t^{r'})/(z^r - z^{r'}) : (z^r, t^r) \in P \text{ with } z^r > z^{r'}\}$. Update $P' = P' \cup \{(z^{r'+1}, t^{r'+1})\}$. Repeat step 2.

Algorithm 2 constructs the k-upper envelope of $\mathcal{L}$ in $O(n_k \log^2|\mathcal{L}|)$ time and $O(n_k|\mathcal{L}| + |\mathcal{L}|)$ space, where n_k denotes the maximum number of edges of the k-upper envelope of any set with $|\mathcal{L}|$ lines (see Edelsbrunner and Welzl 1986). An upper bound on $n_k = O(|\mathcal{L}|k^{\frac{1}{2}})$ can be found in Edelsbrunner and Welzl (1985). Dey (1998), Tóth (2000), and Nivasch (2008) have subsequently improved the upper bound of the complexity of this problem by studying a closely related problem, the k-set problem, in the two-dimensional case. As for the Jarvis march algorithm, in the two-dimensional case presented here, it has running time $O((R+2)(R'+1))$ (Tóth et al. 2017). For detailed results on the complexity of related algorithms and for extensions to the multidimensional case, we refer the reader to Online Section EC.2.

Valid Inequalities (5) and Algorithms 2 and 3 can be generalized to work with finite discrete distributions with unequal probabilities. Observe that the definition of the $(p+1)$-lower ($(p+1)$-upper) envelope is based on satisfying Constraint (4d). In this extension, Constraint (4d) is replaced with $\sum_{s\in\mathcal{S}} p_s y_s \leqslant \epsilon$, where p_s is the probability of scenario s. Hence, it suffices to redefine the lower (upper) score of a point as the probability of the lines that lie below (above) that point and modify the definition of the k-lower (-upper) envelope and step 3 of Algorithm 2 accordingly so that this more general constraint is satisfied.

The following theorem sheds light on the strength of our valid inequalities.

Theorem 1. *Let $\mathcal{FR}_j$ be the feasible region of the relaxation of Problem (4) associated to a given row $j \in \mathcal{J}$, that is,*

$$\min_{x, y_s} \quad f(x) \tag{7a}$$

$$\text{s.t.} \quad (4b), (4d), (4e), \tag{7b}$$

$$\Omega_{js}\hat{a}_j^\top x - b_{js} + x^\top a_j^0 \leqslant M_{js} y_s, \quad \forall s \in \mathcal{S}. \tag{7c}$$

Assuming that the set X of deterministic constraints given in (4b) is nonempty and compact, the set (6) of valid inequalities for all $j \in \mathcal{J}$ provides $\cap_{j\in\mathcal{J}}\text{conv}(\mathcal{FR}_j)$.

The proof of this theorem is a direct consequence of Proposition 2 in Online Section EC.1.

Furthermore, it is possible to relate our valid inequalities with the quantile cuts described in Qiu et al. (2014) and Xie and Ahmed (2018). To see this, consider Problem (4) with feasible region $\mathcal{FR}$ and note that $\mathcal{FR} = \cap_{j\in\mathcal{J}}\mathcal{FR}_j$. The quantile cuts can be viewed as a projection of the well-known family of mixing inequalities in the (x, y)-space onto the original space x. Quantile cuts represent an infinite family of inequalities, and the intersection of all quantile cuts is called the quantile closure. If another round of quantile cuts is applied to a stronger formulation, specifically the original formulation with the (first) quantile closure, a subsequent closure can be derived (the second closure) and so on. In Xie and Ahmed (2018), it is proved that the sequence of sets obtained by successive quantile closure operations converges to the convex hull of the feasible region of the original problem with respect to the Hausdorff metric, $\text{conv}(\mathcal{FR})$. It is also shown that the separation over the first quantile closure is NP-hard. Corollary 1 in Online Section EC.1 shows that the set (6) of valid inequalities (per

Downloaded from informs.org by [2001:720:c20:cc05::40:111] on 07 November 2023, at 08:26 . For personal use only, all rights reserved.

constraint $j \in \mathcal{J}$) coincides with the limit of the succession of quantile closures of $\mathcal{FR}_j$ as the order of the closure grows to infinity. This limit is precisely $\text{conv}(\mathcal{FR}_j)$.

3. Optimal Power Flow Under Uncertainty: A Joint Chance-Constrained Modeling Approach

The OPF is a routine at the core of important tools for power system operations (Frank et al. 2012). In its deterministic version, the OPF problem seeks to determine the least costly dispatch of thermal generating units to satisfy the system's net demand (i.e., demand minus renewable generation), complying with the technical limits of production and transmission network equipment. The main challenge of the OPF is that it is a nonlinear and nonconvex optimization problem because of the power flow equations that govern the (static) behavior of power systems. For this reason, the DC approximation of the power flow equations, which transforms the problem into a linear program, is frequently used. The demand and renewable generation are factors that increase the uncertainty in power systems, and ignoring it can lead to unsafe operating conditions.

However, given the inherently uncertain nature of the electricity net demand, the probabilistic version of the OPF problem can be formulated as a JCCP that aims at minimizing the expected production cost, enforcing that the technical constraints are satisfied with a given (high) probability. In this context, chance-constrained programming can be used to minimize the expected operating cost, guaranteeing that the system withstands unforeseen peaks of electrical load because of stochastic demand or uncertainty in power generation (Van Ackooij et al. 2011). The chance-constrained OPF (CC-OPF) problem addresses this uncertainty and pursues ensuring the safe operation of a power system with a high level of probability.

To address the CC-OPF problem, several papers in the literature (e.g., Roald and Andersson 2018) directly work with SCCs. However, the main drawback of this modeling approach is that, even in those cases in which the probability of violating each individual constraint seems more than tolerable, the resulting joint risk (that is, the probability that any of the technical constraints is violated) may still be excessive and inadmissible. This is the key motivation behind the use of JCCs to tackle the CC-OPF problem (see, e.g., Peña-Ordieres et al. 2021).

In this vein, there are several approaches in the literature to solve the JCC-OPF problem. Vrakopoulou et al. (2013) adopt the scenario approach to approximate the solution of the JCC-OPF, whereas Chen et al. (2021) propose a heuristic data-driven method that involves enforcing the satisfaction of the technical constraints for a box of the uncertainty. This box is inferred using one-class support vector clustering, and its size is contingent on the system's desired reliability. Hou and Roald (2020) propose an iterative tuning algorithm to solve a robust reformulation of the JCC-OPF problem. Esteban-Pérez and Morales (2023) introduce a distributionally robust JCC-OPF model that considers contextual information using an ambiguity set based on probability trimmings. To make their model tractable, they resort to the widely known CVaR-based approximation of the JCC.

The aforementioned SAA method is another effective way to solve JCCPs and has the potential to identify OPF solutions with a better cost performance than that of the more conservative solutions delivered by the previous approaches. However, solving the JCC-OPF problem using SAA is challenging because of the presence of binary variables, the number of scenarios required, and the size of the power systems. Lejeune and Dehghanian (2020) propose a methodology to solve the SAA of the JCC-OPF without including the power flow equations into the joint chance-constrained system. To the best of our knowledge, we are the first to efficiently solve the JCC-OPF problem by means of the SAA approach, using an MIP reformulation and including the arduous power flow constraints. Furthermore, unlike the sample-based approach introduced in Peña-Ordieres et al. (2021), which relies on a smooth nonlinear approximation of the JCC-OPF, ours offers optimality guarantees.

3.1. Notation and Problem Formulation

In this section, we present the formulation of the JCC-OPF problem that we consider in the case study. To do so, we introduce the following notation and modeling choices, widely used in the power system domain:

1. Power system: A power system can be represented by a directed graph denoted by $G(\mathcal{N}, \mathcal{L})$, where $\mathcal{N}$ is the set of buses (vertices), indexed by n, and $\mathcal{L}$ is the set of transmissions lines (edges), whose direction is chosen arbitrarily and are indexed by l. To supply the net demand at each bus, the power system is equipped with a set of generators $\mathcal{G}$, indexed by g, where $\mathcal{G}_n$ represents the set of generators at bus n. Note that the energy injected at each bus, derived from the balance between generation and net demand, is transported among the buses through the transmission lines. For illustration, Figure 2 depicts a representation of a power system with three buses, three transmission lines, two generators located at nodes 1 and 2 and one electricity net demand at node 3.

2. Nodal net loads: The (uncertain) electricity net demand at node n, $\tilde{d}_n$, is given by $\tilde{d}_n = d_n - \omega_n$, where d_n is the predicted value and ω_n is the forecast error with a change of sign. This error is modeled as a random variable with zero mean that follows an unknown continuous probability distribution.

Downloaded from informs.org by [2001:720:c20:cc05::40:111] on 07 November 2023, at 08:26 . For personal use only, all rights reserved.

Figure 2. Illustrative Three-Node Power System

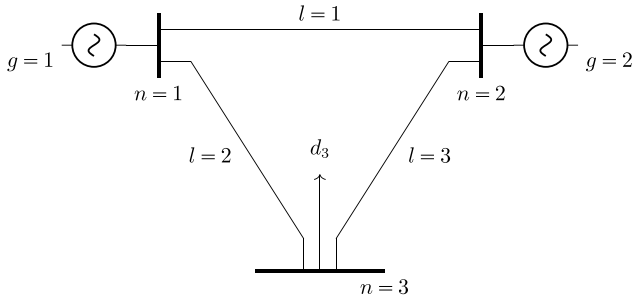

3. Generation: To cope with the forecast errors $(\omega_n)_{n\in\mathcal{N}}$, generators' power outputs are adjusted according to the following affine control policy:

$$\tilde{p}_g = p_g - \beta_g \Omega, \quad \forall g \in \mathcal{G},$$

where $\Omega := \sum_{n\in\mathcal{N}} \omega_n$ is the system-wise aggregated forecast error and p_g and β_g are the power output dispatch and the participation factor of generating unit g, respectively (see, e.g., Bienstock et al. 2014, Hou and Roald 2020, Peña-Ordieres et al. 2021). The minimum and maximum capacity of generator g is denoted by $\underline{p}_g$ and $\overline{p}_g$, respectively.

4. Power balance: Given the affine control policy of the previous point, the power balance equation takes the following form:

$$\sum_{g\in\mathcal{G}} \tilde{p}_g - \sum_{n\in\mathcal{N}} \tilde{d}_n = \sum_{g\in\mathcal{G}} (p_g - \beta_g \Omega) - \sum_{n\in\mathcal{N}} (d_n - \omega_n) = 0.$$

Hence, to ensure the power balance for any realization of the forecast errors $(\omega_n)_{n\in\mathcal{N}}$, it must hold that

$$\sum_{g\in\mathcal{G}} p_g - \sum_{n\in\mathcal{N}} d_n = 0$$
$$\sum_{g\in\mathcal{G}} \beta_g = 1.$$

5. Power flows: Line flows are modeled using the well-known approximation based on the power transfer distribution factors, B_{ln}, $l \in \mathcal{L}$, $n \in \mathcal{N}$, which sets a linear relation between the power flow through line l and the power injected at node n. The maximum capacity of line l is denoted by $\overline{f}_l$.

6. Power production cost: The cost function of each generating unit is assumed to be quadratic, and as a result, the total power production cost is given by

$$\sum_{g\in\mathcal{G}} C_{2,g} (p_g - \Omega\beta_g)^2 + C_{1,g} (p_g - \Omega\beta_g) + C_{0,g},$$

where $C_{2,g}$, $C_{1,g}$, $C_{0,g}$ are the coefficients defining the quadratic cost function of generating unit g. On the assumption that ω_n, for each $n \in \mathcal{N}$, is a random variable with zero mean, we have (see, for instance, Peña-Ordieres et al. 2021)

$$\mathbb{E}\left[\sum_{g\in\mathcal{G}} C_{2,g} (p_g - \Omega\beta_g)^2 + C_{1,g} (p_g - \Omega\beta_g) + C_{0,g}\right] = \sum_{g\in\mathcal{G}} C_{2,g} p_g^2 + C_{1,g} p_g + C_{0,g} + \mathbb{V}(\Omega) C_{2,g} \beta_g^2,$$

where $\mathbb{V}(\Omega)$ denotes the variance of the random variable Ω.

With these ingredients, the JCC-OPF problem we tackle in this paper is formulated as follows:

$$\min_{p_g, \beta_g \geq 0, \forall g\in\mathcal{G}} \quad \sum_{g\in\mathcal{G}} C_{2,g} p_g^2 + C_{1,g} p_g + C_{0,g} + \mathbb{V}(\Omega) C_{2,g} \beta_g^2 \tag{8a}$$

$$\text{s.t.} \quad \sum_{g\in\mathcal{G}} \beta_g = 1, \tag{8b}$$

$$\sum_{g\in\mathcal{G}} p_g - \sum_{n\in\mathcal{N}} d_n = 0, \tag{8c}$$

$$\underline{p}_g \leqslant p_g \leqslant \overline{p}_g, \quad \forall g \in \mathcal{G}, \tag{8d}$$

$$-\overline{f}_l \leqslant \sum_{n\in\mathcal{N}} B_{ln}\left(\sum_{g\in\mathcal{G}_n} p_g - d_n\right) \leqslant \overline{f}_l, \quad \forall l \in \mathcal{L}, \tag{8e}$$

$$\mathbb{P}\left(\begin{array}{l} \underline{p}_g \leqslant p_g - \Omega\beta_g \leqslant \overline{p}_g, \quad \forall g \in \mathcal{G} \\ -\overline{f}_l \leqslant \sum_{n\in\mathcal{N}} B_{ln}\left(\sum_{g\in\mathcal{G}_n}(p_g - \Omega\beta_g) + \omega_n - d_n\right) \leqslant \overline{f}_l, \quad \forall l \in \mathcal{L} \end{array}\right) \geqslant 1-\epsilon. \tag{8f}$$

Objective (8a) is the minimization of the expected total generation cost. The equality Constraints (8b) and (8c) enforce the power balance in the system, whereas Constraints (8d) and (8e) ensure a feasible power dispatch that corresponds to an error-free scenario, that is, to a realization of the net-load forecast errors such that $\omega_n = 0$ $\forall n \in \mathcal{N}$. Finally, Expression (8f) constitutes the joint chance-constraint system by which the decision maker states that the OPF solution must be feasible with a probability greater than or equal to $1-\epsilon$. Accordingly, parameter ϵ is the maximum allowed probability of constraint violation set by the user. Formulation (8) is quite standard and has been used before by Bienstock et al. (2014), Hou and Roald (2020), and Peña-Ordieres et al. (2021), among others.

Problem (8) can be written in the form of (1), that is, as a CCP with linear JCC and random RHS and LHS. To see this, define the vector of continuous decision variables x in (1) as $x := (p_g, \beta_g)_{g\in\mathcal{G}}$ and group all these variables by means of the set $\mathcal{I}$ with elements i running from 1 to $|\mathcal{I}| = 2|\mathcal{G}|$. In this way, we have that $x \in \mathbb{R}_+^{|\mathcal{I}|}$, the set $X \subseteq \mathbb{R}^{|\mathcal{I}|}$ represents the polyhedron defined by the deterministic Constraints (8b)–(8e), and $f : \mathbb{R}^{|\mathcal{I}|} \to \mathbb{R}$ is the convex function providing the expected total generation cost (8a). Likewise, if we collect all the constraints involved in the joint chance-constraint system (8f) into the set $\mathcal{J}$ (hence, $|\mathcal{J}| = 2|\mathcal{G}| + 2|\mathcal{L}|$), this system can be represented by way of a technology matrix with random rows $a_j(\omega) \in \mathbb{R}^{|\mathcal{I}|}$, $j \in \mathcal{J}$, and random RHS $b_j(\omega) \in \mathbb{R}$, $j \in \mathcal{J}$, where the uncertainty is again represented through the random vector ω taking values in $\mathbb{R}^{|\mathcal{N}|}$.

As discussed in Section 2, the CCP (8) can be easily reformulated into an MIP using SAA. Thus, we assume that ω has a finite discrete support defined by a collection of points $\{\omega_s \in \mathbb{R}^{|\mathcal{N}|}, s \in \mathcal{S}\}$ and respective probability masses $\mathbb{P}(\omega = \omega_s) = (1/|\mathcal{S}|)$, $\forall s \in \mathcal{S} = \{1, \ldots, |\mathcal{S}|\}$. Accordingly, ω_{ns} and Ω_s are realizations of the respective random variables under scenario s. We define $p := \lfloor \epsilon|\mathcal{S}| \rfloor$, the vector y of binary variables y_s, $\forall s \in \mathcal{S}$, and the large enough constants $M^1_{gs}, M^2_{gs}, M^3_{ls}, M^4_{ls}$. Thus, the MIP reformulation of Problem (8) is written as follows:

$$\min_{p_g, \beta_g \geqslant 0, y_s} \quad \sum_{g\in\mathcal{G}} C_{2,g}\, p_g^2 + C_{1,g}\, p_g + C_{0,g} + \hat{\mathbb{V}}(\Omega)\, C_{2,g}\, \beta_g^2 \tag{9a}$$

$$\text{s.t.} \quad (8b) - (8e), \tag{9b}$$

$$p_g - \Omega_s\beta_g \geqslant \underline{p}_g - y_s M^1_{gs}, \quad \forall g \in \mathcal{G}, s \in \mathcal{S}, \tag{9c}$$

$$p_g - \Omega_s\beta_g \leqslant \overline{p}_g + y_s M^2_{gs}, \quad \forall g \in \mathcal{G}, s \in \mathcal{S}, \tag{9d}$$

$$\sum_{n\in\mathcal{N}} B_{ln}\left(\sum_{g\in\mathcal{G}_n}(p_g - \Omega_s\beta_g) - d_n + \omega_{ns}\right) \geqslant -\overline{f}_l - y_s M^3_{ls}, \quad \forall l \in \mathcal{L}, s \in \mathcal{S}, \tag{9e}$$

$$\sum_{n\in\mathcal{N}} B_{ln}\left(\sum_{g\in\mathcal{G}_n}(p_g - \Omega_s\beta_g) - d_n + \omega_{ns}\right) \leqslant \overline{f}_l + y_s M^4_{ls}, \quad \forall l \in \mathcal{L}, s \in \mathcal{S}, \tag{9f}$$

$$\sum_{s\in\mathcal{S}} y_s \leqslant p, \tag{9g}$$

$$y_s \in \{0,1\}, \quad \forall s \in \mathcal{S}. \tag{9h}$$

Constraints (9c)–(9f) represent the sample-based reformulation of the joint chance constraint (8f). For a given scenario $s \in \mathcal{S}$, Inequalities (9c)–(9f) guarantee that all the original constraints are satisfied when $y_s = 0$. If $y_s = 1$, some of the original constraints can be violated for scenario s. Finally, Inequality (9g) ensures that the probability of the JCC is met, and the binary character of variables y_s is declared in (9h).

3.2. Numerical Experiments

This section discusses a series of numerical experiments with which we evaluate the different approaches presented in Section 2 to solve the SAA-based MIP reformulation of the JCC-OPF. In particular, we compare the performance of approaches **T**, **TS**, and **TS+V** using five standard power systems widely employed in the technical

Downloaded from informs.org by [2001:720:c20:cc05::40:111] on 07 November 2023, at 08:26 . For personal use only, all rights reserved.

Downloaded from informs.org by [2001:720:c20:cc05::40:111] on 07 November 2023, at 08:26 . For personal use only, all rights reserved.

Table 1. Short Description of Test Power Systems

	IEEE-RTS-24	IEEE-57	IEEE-RTS-73	IEEE-118	IEEE-300
Number of nodes	24	57	73	118	300
Number of generators	32	4	96	19	57
Number of lines	38	41	120	186	411

literature on the topic, namely, the IEEE-RTS-24, IEEE-57, IEEE-RTS-73, IEEE-118, and IEEE-300 test systems. All data pertaining to these systems are publicly available in the repository Power Grid Lib (2022) under version 21, and their main features are listed in Table 1. All optimization problems were solved using GUROBI 9.1.2 (Gurobi Optimization, LLC 2022) on a Linux-based server with CPUs clocking at 2.6 GHz, 6 threads and 32 GB of RAM. In all cases, the optimality GAP has been set to 10^{-9}% and the time limit to 10 hours. All data used and codes implemented throughout these numerical experiments can be found in the repository OASYS (2023).

Similarly to Peña-Ordieres et al. (2021), we assume that the error of net loads is normally distributed, that is, $\omega \sim N(\mathbf{0}, \Sigma)$, where $\mathbf{0}$ and Σ represent, respectively, the zero vector and the covariance matrix. We also assume that the standard deviation of ω_n at node n is proportional to the net nodal demand d_n according to a parameter ζ between zero and one. Thus, this parameter controls the magnitude of net demand fluctuations. Under these assumptions, the procedure to model uncertainty proposed in Peña-Ordieres et al. (2021) runs as follows. First, we compute the positive definite matrix $C = \hat{C}\hat{C}^{\top}$, where each element of matrix $\hat{C}$ is a sample randomly drawn from a uniform distribution with support in $[-1, 1]$. Then, to obtain a positive definite matrix Σ in which the diagonal elements are equal to $(\zeta d_n)^2$, we define each of its entries ($\sigma_{nn'}$) as follows:

$$\sigma_{nn'} = \zeta^2 \frac{c_{nn'}}{\sqrt{c_{nn} c_{n'n'}}} d_n d_{n'}, \quad \forall n, n' \in \mathcal{N},$$

where $c_{nn'}$ denotes the element of matrix C in row n and column n'. To avoid generating infeasible instances of the JCC-OPF problem, the parameter ζ has been set to 0.15 for the four smallest systems and to 0.05 for the IEEE-300 system. To characterize the net demand uncertainty, we consider 1,000 scenarios and a tolerable probability of violation of the joint chance constraint of 5% (i.e., $\epsilon = 0.05$ and $p = 50$). Finally, each solution strategy is run for 10 different sets of randomly generated samples. Accordingly, in this section, we provide tables with figures averaged over these 10 instances. Also, the generated samples can be downloaded from the repository OASYS (2023).

Table 2 includes the results of solving the mixed-integer quadratic optimization Model (9) if the large constants M^1_{gs}, M^2_{gs}, M^3_{ls} and M^4_{ls} are set to a high enough arbitrary value, specifically 10^4. Despite being remarkably computationally expensive, this approach is used in the technical literature (e.g., Zhang et al. 2015), and thus, we refer to it as the benchmark approach (**BN**). Table 2 includes the number of constraints in the model (#CON), the linear relaxation gap (LR-GAP) calculated using the optimal solution of each instance, the optimality gap given by the difference between the best lower bound and the best integer solution found by the MIP solver (MIP-GAP), the number of instances solved to global optimality in less than 10 hours (#OPT), and the solution time in seconds (time). As expected, the computational time needed to solve the OPF with the Big M Model (9) increases significantly with the size of the instances. Whereas the 10 instances from systems IEEE-RTS-24, IEEE-57, and IEEE-73 are solved in less than 10 hours, none of the instances for systems IEEE-118 and IEEE-300 are solved to global optimality within that time limit, and the average MIP-GAP after 10 hours amounts to 0.29% and 0.27%, respectively. Interestingly, despite that the LR-GAP is relatively low for the IEEE-RTS-73 system, the average computational time required to solve this case is particularly high compared with the two smaller systems.

As discussed in the technical literature, a proper tuning of the Big-Ms makes Model (9) tighter and generally easier to solve (Qiu et al. 2014) by the MIP routine. Therefore, we evaluate the computational performance of the iterative coefficient strengthening algorithm and provide the corresponding results in Table 3. In particular, **T**(1), **T**(2), and **T**(3) represent the results obtained by solving Model (9) with the Big M values provided by Algorithm

Table 2. Benchmark Approach (**BN**): Results

	IEEE-RTS-24	IEEE-57	IEEE-RTS-73	IEEE-118	IEEE-300
#CON	140,143	168,171	432,435	410,413	936,939
LR-GAP, %	1.756	0.623	0.061	0.956	1.114
MIP-GAP, % (#OPT)	0.00 (10)	0.00 (10)	0.00 (10)	0.29 (0)	0.27 (0)
Time, s	1,121.3	103.2	11,161.2	36,000.0	36,000.0

Downloaded from informs.org by [2001:720:c20:cc05::40:111] on 07 November 2023, at 08:26 . For personal use only, all rights reserved.

Table 3. Coefficient Tightening Approach (**T**): Results

		IEEE-RTS-24	IEEE-57	IEEE-RTS-73	IEEE-118	IEEE-300
LR-GAP, %	**T**(1)	1.755	0.510	0.061	0.711	0.472
	T(2)	1.662	0.330	0.055	0.522	0.324
	T(3)	1.386	0.255	0.029	0.434	0.264
MIP-GAP, % (#OPT)	**T**(1)	0.00 (10)	0.00 (10)	0.00 (10)	0.27 (0)	0.16 (0)
	T(2)	0.00 (10)	0.00 (10)	0.03 (2)	0.16 (0)	0.09 (0)
	T(3)	0.00 (10)	0.00 (10)	0.00 (10)	0.12 (0)	0.07 (0)
Speedup factor	**T**(1)	0.22×	0.07×	0.61×	1.00×	1.00×
	T(2)	0.17×	0.13×	0.31×	1.00×	1.00×
	T(3)	0.48×	0.24×	0.66×	1.00×	1.00×

1 with $\kappa = 1, 2$, and 3, respectively. Table 3 includes the average values of LR-GAP and MIP-GAP, the number of instances solved to optimality in less than 10 hours (#OPT), and the speedup factor with respect to the benchmark approach. To determine this factor, we consider that the total computational time of approach **T** is given as the sum of the time required to run Algorithm 1 κ times to determine the Big-Ms plus the time it takes to solve Problem (9).

Because reducing the Big M values makes Model (9) tighter, the results in Table 3 show lower values of LR-GAP with respect to **BN**. Furthermore, this effect grows with the number of iterations because Algorithm 1 ensures that the Big-Ms never increase between iterations. Although decreasing the values of the Big-Ms leads to tighter MIPs for all the test systems, the numerical results in Table 3 clearly indicate that computational savings are not guaranteed in all cases. Indeed, whereas the 10 instances are solved by **BN** in less than 10 hours for the IEEE-RTS-73 system, **T**(2) only provides the optimal solution for two instances. On top of that, the speedup factors for the three smaller systems are always lower than one, which means that the computational times actually increase in these cases. On the contrary, the average MIP-GAP of the two largest systems is significantly decreased with respect to **BN**. Therefore, we conclude that, because of the heuristics implemented in current commercial MIP solvers, the computational advantages that one could expect a priori from iterative coefficient strengthening are not always guaranteed and are contingent on the structure and data of the problem.

Next, in Table 4, we provide the computational results related to the **TS** method, in which Algorithm 1 is extended to remove redundant constraints from Model (9). Here, #CON is provided as the percentage of the number of constraints of the reference model **BN** (indicated in Table 2) that are retained by **TS** in each iteration. Table 4 also includes the average MIP-GAP, the number of instances solved to optimality and the average speedup factor in relation to **BN**.

Table 4 shows that the upgraded Algorithm 1 screens out a large percentage of the constraints in Model (9), only retaining between 2% and 26% of them. The results in this table demonstrate that combining the tightening of the Big-Ms and the elimination of superfluous constraints leads to significant computational savings. For instance, the speedup factor for the three smallest systems ranges now between 1.5 and 15.1 times. In addition, **TS**(3) is able to solve six and four instances to optimality for systems IEEE-118 and IEEE-300, respectively, in less than 10 hours, and the average MIP-GAP is reduced to 0.01% in these two largest power systems. Therefore, the computational performance of Model (9) is drastically improved by combining the strengthening of the Big -Ms (making Model (9) tighter) and the removal of redundant constraints (making Model (9) more compact). Equally important, the elimination of superfluous constraints notably reduces the MIP solver's need for RAM memory, which decreases from around 100 GB in **T** to 32 GB in **TS**.

Table 4. Tightening and Screening (**TS**): Results

		IEEE-RTS-24	IEEE-57	IEEE-RTS-73	IEEE-118	IEEE-300
#CON, %	**TS**(1)	23.9	2.8	26.0	8.9	12.7
	TS(2)	23.3	2.2	23.8	6.3	9.1
	TS(3)	23.1	2.1	23.0	5.6	8.0
MIP-GAP, % (#OPT)	**TS**(1)	0.00 (10)	0.00 (10)	0.00 (10)	0.15 (0)	0.08 (0)
	TS(2)	0.00 (10)	0.00 (10)	0.00 (10)	0.03 (2)	0.04 (0)
	TS(3)	0.00 (10)	0.00 (10)	0.00 (10)	0.01 (6)	0.01 (4)
Speedup factor	**TS**(1)	1.5×	1.8×	4.7×	1.0×	1.0×
	TS(2)	1.5×	3.8×	2.6×	1.1×	1.0×
	TS(3)	3.8×	4.4×	15.1×	1.4×	1.2×

Downloaded from informs.org by [2001:720:c20:cc05::40:111] on 07 November 2023, at 08:26 . For personal use only, all rights reserved.

Table 5. Tightening by Valid Inequalities (**BN+V**): Results

	IEEE-RTS-24	IEEE-57	IEEE-RTS-73	IEEE-118	IEEE-300
#CON, %	101.0	101.2	101.2	101.6	101.5
LR-GAP, %	0.3374	0.2038	0.0001	0.4784	0.3192
MIP-GAP, % (#OPT)	0.00 (10)	0.00 (10)	0.00 (10)	0.03 (1)	0.08 (0)
Speedup factor	46.4×	13.8×	65.2×	1.1×	1.0×

We continue the numerical experiments by evaluating the impact of including the valid inequalities derived in Section 2.2 in Model (9). The so-obtained results are collated in Table 5. In what follows, this approach is called **BN+V** for short. The results in Table 5 comprise, in order and following the previous notation, the average number of constraints, the average values of LR-GAP and MIP-GAP, the number of instances solved to optimality, and the average speedup factor with respect to the **BN** approach of Table 2.

As can be seen, our valid inequalities only increase the total number of constraints by 1.0%–1.6%. However, the LR-GAP is significantly reduced compared with that obtained by **BN**. This effect is particularly noticeable for the IEEE-RTS-73 system with an average value of the linear relaxation gap equal to 0.0001%, meaning that the linear relaxation of Problem (9) with the proposed valid inequalities is very tight and its solution very close to the actual solution of that problem. Furthermore, the inclusion of the valid inequalities leads to average speedup factors that range between 13.8 and 65.2 times for the three smallest systems. For the two largest systems, the time limit is reached in most instances, but the average MIP-GAP is reduced to 0.03% and 0.08%, respectively.

Finally, we present similar simulation results for the setup in which the valid inequalities are also used to boost the tightening and screening power of Algorithm 1 (that is, the valid inequalities are also included in Problem (3)), leading to method **TS+V**. Table 6 provides the average number of constraints, the average values of LR-GAP and MIP-GAP, and the average speedup factor of **TS+V** with respect to **BN** in Table 2. Because increasing the number of iterations of Algorithm 1 barely affects the performance of **TS+V**, all the data shown in Table 6 correspond to $\kappa = 1$.

The comparison of the results in Tables 4–6 yields the following observations. First, including the valid inequalities in Algorithm 1 strengthens the Big-Ms even further, which, in turn, remarkably reduces the linear relaxation gap and increases the number of constraints identified as redundant in Model (9). Indeed, the total number of constraints eventually retained by **TS+V** ranges between 1.61% and 3.84% if compared with **BN**. Second, **TS+V** can solve the 10 instances to global optimality in less than 10 hours for the five test systems considered in these numerical experiments. In fact, the optimal solutions obtained by **TS+V** are the ones we use to compute the values of the linear relaxation gap throughout these simulations. Third, **TS+V** is able to achieve speedup factors between 8.5 and 1,470.0 times, depending on the test system. All in all, **TS+V** features the best computational performance in terms of resolution time and MIP-GAP among all the methods tested so far.

Next, in Table 7, the results of **TS+V** are contrasted with those provided by state-of-the-art approximations available in the literature. In particular, we consider the CVaR-based and ALSO-X conservative approximations, both described in Jiang and Xie (2022). Table 7 provides the average cost increase in percentage with respect to the optimal cost and the speedup factor with regard to **BN** for the different methodologies compared. As expected, the CVaR-based approximation leads to conservative results and involves average cost increases that range between 0.49% and 2.88%. Interestingly enough, **TS+V** computes the optimal solution and involves a higher speedup factor than the CVaR-based approach for two of the five systems. Compared with the two ALSO-X approximations, **TS+V** obtains the global optimal solution in all cases with speedup factors that are still tantamount to those of these approximate methods.

To conclude this study, we compare our solution approach with the one proposed in Luedtke (2014). This author presents an exact approach to solve CCPs based on the addition of quantile cuts in a so-called lazy fashion to a relaxation of the problem that only includes the deterministic constraints. In this way, at each node of the branching tree, we seek a violated constraint from a scenario s with $y_s = 0$. Using the coefficients of this violated

Table 6. Tightening and Screening with Valid Inequalities (**TS+V**): Results

	IEEE-RTS-24	IEEE-57	IEEE-RTS-73	IEEE-118	IEEE-300
#CON, %	3.49	1.61	3.84	2.68	3.30
LR-GAP, %	0.3365	0.1519	0.0001	0.2821	0.1603
MIP-GAP, % (#OPT)	0.00 (10)	0.00 (10)	0.00 (10)	0.00 (10)	0.00 (10)
Speedup factor	706.8×	35.3×	1470.0×	23.1×	8.5×

Downloaded from informs.org by [2001:720:c20:cc05::40:111] on 07 November 2023, at 08:26 . For personal use only, all rights reserved.

Table 7. Comparison of the Proposed **TS+V** Approach and Existing Approximate Methods

		IEEE-RTS-24	IEEE-57	IEEE-RTS-73	IEEE-118	IEEE-300
Average cost increase, %	**TS+V**	0.00	0.00	0.00	0.00	0.00
	CVaR	2.88	0.53	1.71	0.57	0.49
	ALSO-X	0.80	0.08	0.41	0.08	0.05
	ALSO-X+	0.53	0.07	0.12	0.05	0.04
Speedup factor	**TS+V**	706.8×	35.3×	1,470.0×	23.1×	8.5×
	CVaR	387.1×	117.0×	265.1×	4,045.5×	779.7×
	ALSO-X	18.0×	1.2×	21.3×	148.6×	11.13×
	ALSO-X+	7.8×	0.7×	6.6×	49.3×	3.7×

constraint, a valid inequality is derived by means of the resolution of $|\mathcal{S}|$ linear separation subproblems. These strengthened cuts contain binary variables associated to several scenarios and are obtained by applying the star inequalities of Atamtürk et al. (2000).

We implement the procedure, including, at each iteration, both the initial or base violated inequality and the strengthened one because this approach delivered the best results. The comparison between our approach and Luedtke's (which we name BCD for short, from branch-and-cut decomposition) is shown in Table 8. As can be seen, a similar number of constraints are generated in the BCD approach (that includes the deterministic constraints and the cuts generated dynamically). Furthermore, our procedure clearly outperforms the BCD approach in terms of computational time. One possible explanation, already pointed out in the paper, is that the generation of the cuts requires solving 1,000 subproblems at each iteration. In the particular application presented in Luedtke (2014), however, this potential bottleneck is overcome by leveraging the specific structure of the subproblem to develop a closed-form expression of its solution, thus avoiding the need to optimize over all the scenario sets. With that said, we remark that the times provided in Table 8 under the acronym BCD-P correspond to a parallel implementation of the BCD algorithm in which only the time required to solve the most time-consuming subproblem out of the 1,000 to be solved at each iteration is added to the final solution time reported. For completeness and because the parallel implementation of BCD using off-the-shelf optimization solvers is not trivial at all, we also report in Table 8 the speedup factor that is attained by a serial implementation of BCD, termed BCD-S in the table. As can be seen, this implementation is, however, far from being competitive in all cases.

4. Conclusions and Future Research

In this paper, we propose a novel exact resolution technique for an MIP SAA-based reformulation of joint chance-constrained problems in the form of (1). Our methodology includes a screening method to eliminate superfluous constraints based on an iterative procedure to repeatedly tighten the Big-Ms present in the MIP. These procedures are combined with the addition of inequalities that are valid provided that the technology matrix in the chance-constraint system exhibits the structure presented in (4). Said inequalities strengthen the linear relaxation of the MIP SAA-based reformulation and allow for additional screening of constraints. The resultant model is, thus, compact and tight.

We apply our methodology to solve the joint chance-constrained DC optimal power flow. In the case study, we show that, in comparison with the benchmark model, our methodology provides remarkable results in terms of the linear relaxation bounds, the RAM memory needed to solve the instances, and the total computational resolution time. Specifically, our method **TS+V** solves to optimality all the instances generated for the IEEE-RTS-118 and IEEE-RTS-300 test systems, the majority of which are not solved within 10 hours of computational time using the benchmark approach. Furthermore, the average number of constraints eliminated from all instances

Table 8. Comparison of the Proposed **TS+V** Approach and the BCD Approach

		IEEE-RTS-24	IEEE-57	IEEE-RTS-73	IEEE-118	IEEE-300
#CONS, %	**TS+V**	3.49	1.61	3.84	2.68	3.30
	BCD	11.37	2.69	3.58	2.46	1.53
Speedup factor	**TS+V**	706.8×	35.3×	1,470.0×	23.1×	8.5×
	BCD-P	10.12×	2.05×	69.00×	9.24×	4.74×
	BCD-S	0.12×	0.04×	0.30×	1.45×	0.42×

Downloaded from informs.org by [2001:720:c20:cc05::40:111] on 07 November 2023, at 08:26 . For personal use only, all rights reserved.

with **TS+V** always exceeds 95% of them, and the lower bound is markedly increased by the inclusion of the valid inequalities, showing the outstanding results of the combination of the methods developed.

The comparison of our results with those provided by existing approximate and exact methods shows that our approach is computationally very competitive for small and medium-sized instances, always providing the best results in terms of cost. For the large instances addressed, whereas outperformed by the approximate methods in terms of computational time (as expected), our exact solution strategy not only provides a certificate of optimality, but also returns the optimal solution within the set time limit. A promising future research line consists of the development of a generalized set of valid inequalities that combine variables from pairs or subgroups of constraints $j \in \mathcal{J}$ in the chance-constrained system (1c).

Acknowledgments

The authors thankfully acknowledge the computer resources, technical expertise, and assistance provided by the Supercomputing and Bioinformatics Center of the University of Málaga.

References

Abdi A, Fukasawa R (2016) On the mixing set with a knapsack constraint. *Math. Programming* 157(1):191–217.
Ahmed S, Xie W (2018) Relaxations and approximations of chance constraints under finite distributions. *Math. Programming* 170(1):43–65.
Ahmed S, Luedtke J, Song Y, Xie W (2017) Nonanticipative duality, relaxations, and formulations for chance-constrained stochastic programs. *Math. Programming* 162(1):51–81.
Atamtürk A, Nemhauser GL, Savelsbergh MWP (2000) Conflict graphs in solving integer programming problems. *Eur. J. Oper. Res.* 121(1):40–55.
Ben-Tal A, Nemirovski A (2000) Robust solutions of linear programming problems contaminated with uncertain data. *Math. Programming* 88(3):411–424.
Bienstock D, Chertkov M, Harnett S (2014) Chance-constrained optimal power flow: Risk-aware network control under uncertainty. *SIAM Rev.* 56(3):461–495.
Cheema MA, Shen Z, Lin X, Zhang W (2014) A unified framework for efficiently processing ranking related queries. Amer-Yahia S, Christophides V, Kementsietsidis A, Garofalakis M, Idreos S, Leroy V, eds. *Advances in Database Technology - EDBT 2014: 17th Internat. Conf. Extending Database Technology* (OpenProceedings.org, Konstanz, Germany), 427–438.
Chen G, Zhang H, Hui H, Song Y (2021) Scheduling HVAC loads to promote renewable generation integration with a learning-based joint chance-constrained approach. Preprint, submitted December 18, https://arxiv.org/abs/2112.09827.
Conforti M, Cornuéjols G, Zambelli G (2014) *Integer Programming*, vol. 271 (Springer, Cham, Switzerland).
Daníelsson J, Jorgensen BN, de Vries CG, Yang X (2008) Optimal portfolio allocation under the probabilistic VaR constraint and incentives for financial innovation. *Ann. Finance* 4(3):345–367.
Dentcheva D, Prékopa A, Ruszczynski A (2000) Concavity and efficient points of discrete distributions in probabilistic programming. *Math. Programming* 89(1):55–77.
Dey TK (1998) Improved bounds for planar *k*-sets and related problems. *Discrete Comput. Geometry* 19(3):373–382.
Edelsbrunner H, Welzl E (1985) On the number of line separations of a finite set in the plane. *J. Combin. Theory Ser. A* 38(1):15–29.
Edelsbrunner H, Welzl E (1986) Constructing belts in two-dimensional arrangements with applications. *SIAM J. Comput.* 15(1).
Elçi Ö, Noyan N, Bülbül K (2018) Chance-constrained stochastic programming under variable reliability levels with an application to humanitarian relief network design. *Comput. Oper. Res.* 96:91–107.
Esteban-Pérez A, Morales JM (2023) Distributionally robust optimal power flow with contextual information. *Eur. J. Oper. Res.* 306(3):1047–1058.
Frank S, Steponavice I, Rebennack S (2012) Optimal power flow: A bibliographic survey I. *Energy Systems* 3(3):221–258.
Günlük O, Pochet Y (2001) Mixing mixed-integer inequalities. *Math. Programming* 90(3):429–457.
Gurobi Optimization, LLC (2022) Gurobi optimizer reference manual. Accessed July, 2023, https://www.gurobi.com.
Henrion R (2007) Structural properties of linear probabilistic constraints. *Optim.* 56(4):425–440.
Henrion R, Strugarek C (2011) Convexity of chance constraints with dependent random variables: The use of copulae. *Stochastic Optimization Methods in Finance and Energy* (Springer, New York), 427–439.
Hong LJ, Yang Y, Zhang L (2011) Sequential convex approximations to joint chance constrained programs: A Monte Carlo approach. *Oper. Res.* 59(3):617–630.
Hou AM, Roald LA (2020) Chance constraint tuning for optimal power flow. *Internat. Conf. Probab. Methods Appl. Power Systems*, 1–6.
Jiang N, Xie W (2022) ALSO-X and ALSO-X+: Better convex approximations for chance constrained programs. *Oper. Res.* 70(6):3581–3600.
Küçükyavuz S, Jiang R (2022) Chance-constrained optimization under limited distributional information: A review of reformulations based on sampling and distributional robustness. *EURO J. Comput. Optim.* 10:100030.
Lagoa CM, Li X, Sznaier M (2005) Probabilistically constrained linear programs and risk-adjusted controller design. *SIAM J. Optim.* 15(3):938–951.
Lejeune MA, Dehghanian P (2020) Optimal power flow models with probabilistic guarantees: A Boolean approach. *IEEE Trans. Power Systems* 35(6):4932–4935.
Luedtke J (2014) A branch-and-cut decomposition algorithm for solving chance-constrained mathematical programs with finite support. *Math. Programming* 146(1–2):219–244.
Luedtke J, Ahmed S (2008) A sample approximation approach for optimization with probabilistic constraints. *SIAM J. Optim.* 19(2):674–699.
Luedtke J, Ahmed S, Nemhauser GL (2010) An integer programming approach for linear programs with probabilistic constraints. *Math. Programming* 122(2):247–272.

Miller BL, Wagner HM (1965) Chance constrained programming with joint constraints. *Oper. Res.* 13(6):930–945.
Nair R, Miller-Hooks E (2011) Fleet management for vehicle sharing operations. *Transportation Sci.* 45(4):524–540.
Najjarbashi A, Lim GJ (2020) A decomposition algorithm for the two-stage chance-constrained operating room scheduling problem. *IEEE Access* 8:80160–80172.
Natarajan K, Pachamanova D, Sim M (2008) Incorporating asymmetric distributional information in robust value-at-risk optimization. *Management Sci.* 54(3):573–585.
Nemirovski A, Shapiro A (2006) Scenario approximations of chance constraints. *Probabilistic and Randomized Methods for Design Under Uncertainty* (Springer, London), 3–47.
Nemirovski A, Shapiro A (2007) Convex approximations of chance constrained programs. *SIAM J. Optim.* 17(4):969–996.
Nivasch G (2008) An improved, simple construction of many halving edges. *Contemporary Math.* 453:299–306.
OASYS (2023) Data and code for a tight and compact model of the SAA-based joint chance-constrained OPF. Accessed July, 2023, https://github.com/groupoasys/TC_SAA_JCC-OPF, https://github.com/groupoasys/TC_SAA_JCC-OPF.
Peña-Ordieres A, Luedtke JR, Wächter A (2020) Solving chance-constrained problems via a smooth sample-based nonlinear approximation. *SIAM J. Optim.* 30(3):2221–2250.
Peña-Ordieres A, Molzahn DK, Roald LA, Wächter A (2021) DC optimal power flow with joint chance constraints. *IEEE Trans. Power Systems* 36(1):147–158.
Power Grid Lib (2022) Accessed July, 2023, https://github.com/power-grid-lib/pglib-opf.
Prékopa A (2003) Probabilistic programming. Ruszczynski A, Shapiro A, eds. *Stochastic Programming*, Handbooks in Operations Research and Management Science, vol. 10 (Elsevier, Amsterdam), 267–351.
Qiu F, Ahmed S, Dey SS, Wolsey LA (2014) Covering linear programming with violations. *INFORMS J. Comput.* 26(3):531–546.
Roald L, Andersson G (2018) Chance-constrained AC optimal power flow: Reformulations and efficient algorithms. *IEEE Trans. Power Systems* 33(3):2906–2918.
Rockafellar RT, Uryasev S (2000) Optimization of conditional value-at-risk. *J. Risk* 2(3):21–41.
Roos T, Widmayer P (1994) *K*-violation linear programming. *Inform. Processing Lett.* 52(2):109–114.
Shapiro A (2003) Monte Carlo sampling methods. Ruszczynski A, Shapiro A, eds. *Stochastic Programming*, Handbooks in Operations Research and Management Science, vol. 10 (Elsevier, Amsterdam), 353–425.
Shaw K, Irfan M, Shankar R, Yadav SS (2016) Low carbon chance constrained supply chain network design problem: A Benders decomposition based approach. *Comput. Indust. Engrg.* 98:483–497.
Song Y, Luedtke JR, Küçükyavuz S (2014) Chance-constrained binary packing problems. *INFORMS J. Comput.* 26(4):735–747.
Sun H, Xu H, Wang Y (2014) Asymptotic analysis of sample average approximation for stochastic optimization problems with joint chance constraints via conditional value at risk and difference of convex functions. *J. Optim. Theory Appl.* 161(1):257–284.
Taleizadeh AA, Niaki STA, Makui A (2012) Multiproduct multiple-buyer single-vendor supply chain problem with stochastic demand, variable lead-time, and multi-chance constraint. *Expert Systems Appl.* 39(5):5338–5348.
Tanner MW, Sattenspiel L, Ntaimo L (2008) Finding optimal vaccination strategies under parameter uncertainty using stochastic programming. *Math. Biosciences* 215(2):144–151.
Tayur SR, Thomas RR, Natraj NR (1995) An algebraic geometry algorithm for scheduling in presence of setups and correlated demands. *Math. Programming* 69(1):369–401.
Tóth CD, O'Rourke J, Goodman JE (2017) *Handbook of Discrete and Computational Geometry* (CRC Press, Boca Raton, FL).
Tóth G (2000) Point sets with many *k*-sets. *Proc. 16th Annual Sympos. Comput. Geometry*, 37–42.
Van Ackooij W, Zorgati R, Henrion R, Möller A (2011) Chance constrained programming and its applications to energy management. *Stochastic Optimization—Seeing the Optimal for the Uncertain*, 291–320.
Vrakopoulou M, Margellos K, Lygeros J, Andersson G (2013) Probabilistic guarantees for the N-1 security of systems with wind power generation. *Reliability and Risk Evaluation of Wind Integrated Power Systems* (Springer, New Delhi), 59–73.
Xie W, Ahmed S (2016) On the quantile cut closure of chance-constrained problems. *Internat. Conf. Integer Programming Combin. Optim.* (Springer, Cham, Switzerland), 398–409.
Xie W, Ahmed S (2018) On quantile cuts and their closure for chance constrained optimization problems. *Math. Programming* 172(1):621–646.
Zhang Y, Shen S, Mathieu JL (2015) Data-driven optimization approaches for optimal power flow with uncertain reserves from load control. *Amer. Control Conf.* (IEEE, Piscataway, NJ), 3013–3018.

Downloaded from informs.org by [2001:720:c20:cc05::40:111] on 07 November 2023, at 08:26 . For personal use only, all rights reserved.